

# ROBUST SLIDING MODE CONTROL FOR UAV FORMATION WITH EXTERNAL DISTURBANCES UNDER EVENT-TRIGGERED STRATEGY

Lihao Wang<sup>1</sup>, Aijun Li<sup>1</sup>, Changqing Wang<sup>1</sup>, Yury Zabolotnov<sup>2</sup>

<sup>1</sup>School of Automation, Northwestern Polytechnical University, Xi'an, 710072, China <sup>2</sup>Samara National Research University, Samara, 443086, Russia

## **Abstract**

Aiming at UAV formation flight trajectory tracking affected by external disturbances and limited communication, this article studies a robust sliding mode formation control law based on event triggering strategy. To suppress external interference, a robust controller is used. In order to reduce communication between adjacent UAVs, a distributed exponential convergence form of sliding mode control scheme based on an event-triggered strategy is designed. Under this scheme, the communication channel only transmits information at the trigger moment determined by the predetermined trigger conditions, and discontinuous communication is realized in the state of discrete updating of the sliding mode surface. According to theoretical analysis, it can be proved that the stability of the closed-loop system. Zeno behavior does not exist. Finally, numerical simulation was applied to verify the effectiveness of the control law.

Keywords: robust sliding mode control, event-triggered strategy, UAV formation, and external disturbances

### 1. Introduction

In recent years, unmanned aerial vehicles (UAVs) have been gradually used in military, scientific, commercial, and civil fields due to their advantages such as lightweight, portability, and flexibility. With the diversification of mission requirements and the complexity of the social production environment, multi-UAV formations have more prominent advantages and capabilities [1]. The communication methods of UAV formation are mainly centralized, distributed, and decentralized [2]. The centralized type has a large amount of interactive data between members and is prone to communication blockage affecting the formation effect and high cost; the decentralized type has no information interaction with each other, and the formation effect is poor; while the distributed control only needs information from local and neighboring agents, and the formation effect is better, with fewer communication needs and lower cost. It is the main communication transmission method used in the research on formation control nowadays [3].

The main control methods for UAV formation are the leader-follower method, the virtual structure method, and the behavior-based method. The leader-follower method means that one UAV is the leader of the whole formation, and the other UAVs are the followers; the leader flies along the preplanned path, and the followers keep a certain spatial geometric distance from the leader and fly along with it. The leader-follower method is currently the most common and mature form of formation control. Many other scholars have completed the experimental validation of UAV formation based on the leader-follower method [4], [5], [6], [7].

Sliding mode control is widely used to deal with uncertain nonlinear systems because of its high reliability in dealing with uncertain parameters, nonlinearity, and external disturbances [8]. The trajectory tracking control problem of the formation system under external disturbance is studied, and the sliding mode controller technology is used to ensure the robustness of the system [9]. Shen Suiyuan et al. proposed a control law design method based on the adaptive neural network extended state observer-based finite-time convergent sliding mode control [10]. Wang et al. designed the sliding mode formation controller, which not only ensures that the linear velocity and angular velocity of the UAV meet the constraints but also relaxes the speed adjustment range of the leader [11].

From the perspective of resource utilization, the above control methods are based on continuous-time trigger control, which undoubtedly causes great waste because some communications are unnecessary. In order to solve this problem, reducing communication frequency has been proposed as an effective method in the past decade. Event-triggered control has been widely used [12]. Guerrero et al. realized the formation test flight of vertical take-off and landing UAVs based on event-driven communication [13]. Yang et al. proposed a state prediction formation algorithm based on an improved dynamic event-driven communication mechanism that can reduce information transmission and ensure high control accuracy of the system [14].

Inspired by the above discussion, this paper adopts the leader-follower method under the distributed structure for the UAV formation problem; in order to make the UAV formation track on the desired trajectory, the sliding mode formation controller is designed by constructing the sliding mode surface containing the formation coordination error to ensure the stability and reliability of the formation; for the external perturbation of the UAV formation, the robust control law is designed to inhibit and process it; and for the problem of the high number of communication between the UAV formation members, the fast update frequency of the controller, and the high consumption of the resources, the event-triggered control strategy is designed to solve it.

# 2. Problem Description

## 2.1 Graph Theory

The communication topology relationship in a UAV formation can be represented by an undirected graph  $G(v,\zeta,A)$ , where  $v=\{v_i,v_2,\cdots,v_n\}$  is the nonempty finite vertex set, representing each member;  $\zeta\subseteq v\times v$  is the edge set, representing the communication links among UAVs; and  $A=[a_{ij}]\in R^{n\times n}$  is the weighted connectivity matrix. If a member  $v_i$  in a UAV formation has access to the state information of a member  $v_j$  through interaction, then there exists an edge pointing from  $v_j$  to  $v_i$  in the graph G, denoted as  $(v_i, v_j) \in \zeta$ .  $v_j$  is said to be a neighbor of  $v_i$ , and there is a corresponding element  $a_{ij}>0$  in the array A, otherwise  $a_{ij}=0$ . In an undirected graph G, the edges are bidirectional, which satisfies  $a_{ij}=a_{ji}$ ; the degree  $c_i(v_i)$  of a vertex  $v_i$  represents the number of neighboring members, and the degree matrix G is a diagonal matrix with the degree  $v_i$  of each vertex as a diagonal element, and its expression is:

$$C = diag\left(c_1(\upsilon_1), c_2(\upsilon_2), \dots, c_n(\upsilon_n)\right) \tag{1}$$

If L is the Laplace matrix of an undirected graph  $G(v,\zeta,A)$ , then the expression for L is as follows:

$$L = C - A \tag{2}$$

where *L* is symmetric and semi-positive definite.

## 2.2 Fixed-Wing UAV Dynamics Model

In a UAV formation, the dynamics model [15] of the *i*-th UAV can be introduced as:

$$\begin{cases} \dot{x}_{i} = V_{i} \cos \theta_{i} \cos \psi_{i} \\ \dot{y}_{i} = V_{i} \cos \theta_{i} \sin \psi_{i} \\ \dot{z}_{i} = V_{i} \sin \theta_{i} \end{cases}$$

$$(3)$$

$$\begin{cases} \dot{V}_{i} = \frac{F_{x_{i}} + d_{il}}{m_{i}} - g \sin \theta_{i} \\ \dot{\theta}_{i} = \frac{F_{y_{i}} - m_{i}g \cos \theta_{i} + d_{i2}}{m_{i}V_{i}} \\ \dot{\psi}_{i} = \frac{F_{z_{i}} + d_{i3}}{m_{i}V_{i} \cos \theta_{i}} \end{cases}$$

$$(4)$$

where i represents the i-th UAV and  $(x_i, y_i, z_i)$  denotes the position in the inertial frame;  $V_i$ ,  $\theta_i$ ,  $\psi_i$  denote the flight speed, flight path angle, and heading angle, respectively;  $(F_{x_i}, F_{y_i}, F_{z_i})$  denotes the control force (including thrust and aerodynamic force) under the track coordinate system;  $(d_{iI}, d_{i2}, d_{i3})$  denotes the external disturbances that the i-th UAV is subjected to in the track coordinate system;  $m_i$  denotes the mass of the i-th UAV, and g denotes the gravitational acceleration.

The position vector, velocity vector, control force vector, disturbance vector, and state vector of the *i*-th UAV are as follows:

$$\boldsymbol{p}_{i} = \left[x_{i}, y_{i}, z_{i}\right]^{T} \tag{5}$$

$$\mathbf{v}_i = \left[x_i, y_i, z_i\right]^T \tag{6}$$

$$\boldsymbol{u}_{i} = \left[F_{xi}, F_{yi}, F_{zi}\right]^{T} \tag{7}$$

$$d_{iN} = [d_{iI}, d_{i2}, d_{i3}]^{T}$$
(8)

$$\boldsymbol{\xi}_{i} = \left[\boldsymbol{p}_{i}, \boldsymbol{v}_{i}\right]^{T} \tag{9}$$

The motion model of the *i*-th UAV can be obtained by combining (3)-(9) as follows:

$$\begin{cases} \dot{\boldsymbol{p}}_i = \boldsymbol{v}_i \\ \dot{\boldsymbol{v}}_i = \boldsymbol{\alpha}_i(\boldsymbol{\xi}_i) + \boldsymbol{\beta}_i(\boldsymbol{\xi}_i)\boldsymbol{u}_i + \boldsymbol{d}_i \end{cases}$$
 (10)

with

$$\boldsymbol{\alpha}_{i}(\boldsymbol{\xi}_{i}) = \begin{bmatrix} 0 \\ 0 \\ -g \end{bmatrix} \tag{11}$$

$$\boldsymbol{\beta}_{i}(\boldsymbol{\xi}_{i}) = \frac{1}{\boldsymbol{m}_{i}} \begin{bmatrix} \cos\theta_{i}\cos\psi_{i} & -\sin\theta_{i}\cos\psi_{i} & -\sin\psi_{i} \\ \cos\theta_{i}\sin\psi_{i} & -\sin\theta_{i}\sin\psi_{i} & \cos\psi_{i} \\ \sin\theta_{i} & \cos\theta_{i} & 0 \end{bmatrix}$$
(12)

$$d_i = \beta_i(\xi_i)d_{iN} \tag{13}$$

Assuming that the UAV formation consists of n UAVs, define the matrix form of each vector in the formation:

$$\boldsymbol{p} = [\boldsymbol{p}_1^T, \boldsymbol{p}_2^T, \cdots \boldsymbol{p}_n^T]^T$$
(14)

$$\mathbf{v} = \left[\mathbf{v}_{1}^{T}, \mathbf{v}_{2}^{T}, \cdots \mathbf{v}_{n}^{T}\right]^{T} \tag{15}$$

$$\boldsymbol{\alpha} = \left[\boldsymbol{\alpha}_{1}^{T}(\boldsymbol{\xi}_{1}), \boldsymbol{\alpha}_{2}^{T}(\boldsymbol{\xi}_{2}), \cdots \boldsymbol{\alpha}_{n}^{T}(\boldsymbol{\xi}_{n})\right]^{T}$$
(16)

The  $\beta(\xi)$  of a formation is defined as a diagonal formation with  $\beta_i(\xi_i)$ :

$$\boldsymbol{\beta}(\boldsymbol{\xi}) = diag(\boldsymbol{\beta}_1^T(\boldsymbol{\xi}_i), \boldsymbol{\beta}_2^T(\boldsymbol{\xi}_i), \cdots \boldsymbol{\beta}_n^T(\boldsymbol{\xi}_i))$$
(17)

The control force vector and disturbance vector in the formation are denoted as follows:

$$\boldsymbol{u} = \left[\boldsymbol{u}_{1}^{T}, \boldsymbol{u}_{2}^{T}, \cdots \boldsymbol{u}_{n}^{T}\right]^{T} \tag{18}$$

$$\boldsymbol{d} = \left[\boldsymbol{d}_{1}^{T}, \boldsymbol{d}_{2}^{T}, \cdots \boldsymbol{d}_{n}^{T}\right]^{T} \tag{19}$$

Then the nonlinear motion model of UAV formation can be expressed as:

$$\begin{cases} \dot{p} = v \\ \dot{v} = \alpha(\xi) + \beta(\xi)u + d \end{cases}$$
 (20)

The position vector and velocity vector of the desired trajectory of the UAV are denoted as  $p_d$  and  $v_d$ , respectively, and the desired state vector  $\xi_d$  is defined as:

$$\boldsymbol{\xi}_{d} = \left[\boldsymbol{p}_{d}, \boldsymbol{v}_{d}\right]^{T} \tag{21}$$

The position error vector and velocity error vector of the *i*-th UAV are denoted as:

$$\boldsymbol{e}_{xi} = \boldsymbol{p}_i - \boldsymbol{p}_d \tag{22}$$

$$e_{vi} = v_i - v_d \tag{23}$$

The position error vector and velocity error vector of the formation are respectively donated as:

$$\boldsymbol{e}_{x} = \left[\boldsymbol{e}_{x1}^{T}, \boldsymbol{e}_{x2}^{T}, \cdots \boldsymbol{e}_{xn}^{T}\right]^{T}$$
(24)

$$\boldsymbol{e}_{v} = \left[\boldsymbol{e}_{vI}^{T}, \boldsymbol{e}_{v2}^{T}, \cdots \boldsymbol{e}_{vn}^{T}\right]^{T}$$
(25)

The state error vector  $\tilde{\xi}_i$  of the *i*-th UAV is denoted as

$$\tilde{\boldsymbol{\xi}}_{i} = \boldsymbol{\xi}_{i} - \boldsymbol{\xi}_{d} = \left[\boldsymbol{e}_{xi}, \boldsymbol{e}_{vi}\right]^{T}$$
(26)

The state error vector of the formation is denoted as

$$\tilde{\boldsymbol{\xi}} = \left[\tilde{\boldsymbol{\xi}}_{1}^{T}, \tilde{\boldsymbol{\xi}}_{2}^{T}, \dots \tilde{\boldsymbol{\xi}}_{n}^{T}\right]^{T} = \left[\boldsymbol{e}_{x}, \boldsymbol{e}_{y}\right]^{T}$$
(27)

Combining (24), (25) and (20), the error model of UAV formation is obtained by derivation:

$$\dot{\boldsymbol{e}}_{x} = \boldsymbol{e}_{v} \tag{28}$$

$$\dot{\mathbf{e}}_{v} = \dot{\mathbf{v}} - \dot{\mathbf{v}}_{d} = \alpha(\xi) + \beta(\xi)\mathbf{u} + \mathbf{d} - \dot{\mathbf{v}}_{d}$$
(29)

Combined with the communication topology between the formation members, the cooperative position error and cooperative speed error of the UAV formation are donated as follows:

$$\boldsymbol{\varepsilon}_{xi} = c_i(\boldsymbol{p}_i - \boldsymbol{p}_d) + \sum_{j=1}^n a_{ij}(\boldsymbol{e}_{xi} - \boldsymbol{e}_{xj})$$
(30)

$$\boldsymbol{\varepsilon}_{vi} = c_i(\boldsymbol{v}_i - \boldsymbol{v}_d) + \sum_{j=1}^n a_{ij}(\boldsymbol{e}_{vi} - \boldsymbol{e}_{vj})$$
(31)

where i, j denote the i-th and j-th UAV in the formation, respectively,  $a_{ij}$  is an element in the weighted connection matrix A of the UAV communication topology, and  $c_i$  is an element in the degree matrix C.

**Remark 1** According to (30) and (31), the UAV formation will track on the desired trajectory and form the desired formation when both cooperative position error  $\varepsilon_{xi}$  and cooperative speed error  $\varepsilon_{yi}$  converge to zero.

#### 2.3 Control Objective

For the trajectory tracking of UAV formation flight affected by external disturbances and

communication constraints, the control objective is to construct a robust sliding mode formation cooperative controller based on an event-triggered strategy.

To achieve the control objective, the following assumptions, properties, and lemmas are used.

**Assumption 1** The external disturbances are assumed to be bounded and slowly varying [16], i.e., they satisfy  $\| \mathbf{d}_{iN} \| \le d_{imax}$ ,  $\dot{\mathbf{d}}_{iN} \approx 0$ ,  $\dot{d}_{imax} = 0$ .

**Definition 1**  $sign(\bullet)$  in all controllers in this paper denotes a sign function, and assuming a vector  $\mathbf{x} = [x_1, x_2, \cdots x_i]^T$ , the expression of the sign function defining the vector  $\mathbf{x}$  is:

$$sign(\mathbf{x}) = \left[sign(x_1), sign(x_2), \cdots sign(x_i)\right]^T$$
(32)

$$sign(x_{i}) = \begin{cases} 1, & x_{i} > 0 \\ 0, & x_{i} = 0 \\ -1, & x_{i} < 0 \end{cases}$$
(33)

## 3. Main Results

## 3.1 Sliding Mode Formation Cooperative Controller Design

According to (30) and (31), the sliding mode surface of the *i*-th UAV is designed to be in exponentially convergent form:

$$\mathbf{s}_{i} = \mathbf{\varepsilon}_{vi} + \lambda \mathbf{\varepsilon}_{xi} \tag{34}$$

where  $\lambda$  is a constant that satisfies the Hurwitz condition and is greater than 0.

Define the sliding mode surface matrix of the UAV formation as:

$$\mathbf{s} = \left[\mathbf{s}_{1}^{T}, \mathbf{s}_{2}^{T}, \cdots \mathbf{s}_{n}^{T}\right]^{T} \tag{35}$$

Considering the communication topology in the UAV formation, and combining the knowledge of graph theory, it can be seen that the communication connectivity of the UAV formation is represented by the graph G. The Laplace matrix of the graph G is L, and C is the degree matrix, then by defining the matrices  $H_I$  and  $H_2$ :

$$H_{I} = (L+C) \otimes I_{3\times 3} = H_{2}^{-1}$$
(36)

where  $\otimes$  denotes the Kronecker product;  $H_1$  and  $H_2$  are mutually inverse matrices, then the sliding mode surface of (34) can be rewritten in the following form:

$$S_i = H_I(e_{vi} + \lambda e_{xi}) \tag{37}$$

The sliding surface and its derivatives of the formation obtained by (28), (29), (35) are as follows:

$$s = H_I(e_v + \lambda e_x) \tag{38}$$

$$H_2 \dot{s} = \alpha(\xi) + \beta(\xi) u + d + \lambda e_v - \dot{v}_d$$
(39)

**Remark 2** Since the formation coordinated position error and coordinated velocity error in the sliding mode surface *s* contain the state information of the neighboring UAVs, the formation coordinated error is updated only when communication between the formation members takes place, and it is possible to determine whether there is continuous communication between the formation members based on whether the sliding mode surface is continuously updated or not.

## 3.2 Robust Controller Design

To compensate for the external disturbances term d, the following robust control law is designed. Assume that  $d_C$  is a vector associated with the boundary of the disturbances d, while the disturbances exist an upper bound  $d_U$  and a lower bound  $d_L$ , i.e., the disturbances d is satisfied:

$$d_L \le d \le d_U \tag{40}$$

Design  $d_{c}$  for:

$$d_{C} = \frac{d_{U} + d_{L}}{2} + \frac{d_{U} - d_{L}}{2} sign(s(t_{k}))$$
(41)

# 3.3 Event-Triggered Strategy Design

The communication channel between the *i*-th UAV and its neighboring UAVs only transmits information at the trigger instants  $t_k$ , which can reduce the consumption of communication resources. The event-triggered function  $f_{COMM}$  for UAV formation communication is:

$$f_{COMM} = //(\lambda - k_2)e_v - s(t_k) // - \eta$$
(42)

where  $\eta$  is the parameter to be designed and satisfies  $0 < \eta < k_I$ .

Define event-triggered error  $e_{COMM}$  for formation communication:

$$e_{COMM} = (\lambda - k_2)e_v - s(t_k)$$
(43)

The event-triggered conditions for designing UAV formation communication are:

$$f_{COMM} > 0 \tag{44}$$

The trigger instants sequence can be defined as

$$t_{k+1} = min\{t > t_k / f_{COMM} > 0\}, k = 0, 1, 2, \dots$$
 (45)

**Remark 3** When the state of the UAV formation error system satisfies (44), the formation members communicate with each other while variables such as the formation coordination error and the sliding mode surface are updated, and the controller uses the updated sliding mode surface to solve the control force. After updating the control forces, the state of the system will re-satisfy the condition  $f_{COMM} > 0$ .

At other moments, when the state of the system does not satisfy the event-triggered conditions, no communication occurs between the formation members. The system always satisfies:

$$/\!/ e_{COMM} /\!/ \leq \eta \tag{46}$$

**Theorem 1** For the UAV formation error system shown in (28)(29), combined with the sliding mode surface and its derivative (38)(39), robust controller (41) and event-triggered mechanism (44), the event-triggered formation cooperative controller is designed as follows:

$$u = \beta^{-1}(\xi)[-\alpha(\xi) - s(t_k) - k_1 sign(s(t_k)) - k_2 e_v - d_C + \dot{v}_d]$$
(47)

where  $k_1$  and  $k_2$  are the controller design parameters, and are constants greater than 0.

Under the control of the event-triggered formation cooperative controller (47), the system can converge asymptotically and stably, and can track the desired trajectory while achieving discontinuous communication. At the same time, Zeno phenomenon will not occur.

**Remark 4** The sliding mode surface  $s(t_k)$  in the controller (47) is updated only when the UAV formation satisfies the event-triggered conditions.  $t_k$  represents the k-th communication moment of the UAV.  $t_k$  in the controller (47) is determined based on the event-triggered conditions, and the update of  $s(t_k)$  represents that the UAVs communicate only at the moment  $t_k$ , and do not communicate at the rest of the moments.

**Remark 5** The controller (47) is continuously updated in each control cycle. If the UAV formation does not communicate in a control cycle, the control update calculation is performed along the value of the previous moment on the sliding mode surface. Since  $\alpha(\xi)$ ,  $\beta(\xi)$ ,  $e_v$  and  $v_d$  in the controller do not contain state variables of neighboring UAVs, these variables can be updated without communication. **Proof.** 

The Lyapunov function is chosen as:

$$V = \frac{1}{2}s^{T}H_{2}s \tag{48}$$

Take the time derivate of (48)

$$\dot{V} = \mathbf{s}^T H_2 \dot{\mathbf{s}} \tag{49}$$

Substituting (39) gives:

$$\dot{V} = \mathbf{s}^{T} \left( \alpha(\xi) + \beta(\xi) \mathbf{u} + \mathbf{d} + \lambda \mathbf{e}_{v} - \dot{\mathbf{v}}_{d} \right) 
= \mathbf{s}^{T} \left( \alpha(\xi) + \beta(\xi) \mathbf{u} + \mathbf{d} - \dot{\mathbf{v}}_{d} \right) + \lambda \mathbf{s}^{T} \mathbf{e}_{v}$$
(50)

Substituting the controller (47) gives:

$$\dot{V} = \sum_{i=1}^{n} (s_i^T \boldsymbol{\alpha}_i(\boldsymbol{\xi}) + s_i^T (-\boldsymbol{\alpha}_i(\boldsymbol{\xi}) - \boldsymbol{s}_i(t_k) - k_I sign(\boldsymbol{s}_i(t_k))) 
- k_2 e_v - d_C + \dot{v}_d) + s_i^T d_i - s_i^T \dot{v}_d + \lambda s_i^T e_v) 
= \sum_{i=1}^{n} (-\boldsymbol{s}_i^T \boldsymbol{s}_i(t_k) - k_I \boldsymbol{s}_i^T sign(\boldsymbol{s}_i(t_k)) + (\lambda - k_2) \boldsymbol{s}_i^T e_v + \boldsymbol{s}_i^T (d_i - d_C))$$
(51)

According to the event-triggered function error (43), this reduces to:

$$\dot{V} = \sum_{i=1}^{n} \left( \mathbf{s}_{i}^{T} \mathbf{e}_{COMM} - k_{I} \mathbf{s}_{i}^{T} sign(\mathbf{s}_{i}(t_{k})) + \mathbf{s}_{i}^{T} (\mathbf{d}_{i} - \mathbf{d}_{C}) \right)$$
(52)

Considering the designed event-triggered condition (46), it is obtained:

$$\dot{V} \leq \sum_{i=1}^{n} ( || s_{i} || || e_{COMM} || -k_{I} s_{i}^{T} sign(s_{i}(t_{k})) + s_{i}^{T} (d_{i} - d_{C}) )$$

$$\leq \sum_{i=1}^{n} ( \eta || s_{i} || -k_{I} s_{i}^{T} sign(s_{i}(t_{k})) + s_{i}^{T} (d_{i} - d_{C}) )$$
(53)

(53) can be expressed in two parts  $\dot{V} \leq \dot{V}_1 + \dot{V}_2$ , where:

$$\dot{V}_{I} = \sum_{i=1}^{n} \left( \eta // s_{i} // -k_{I} s_{i}^{T} sign(s_{i}(t_{k})) \right)$$
(54)

$$\dot{V}_2 = \sum_{i=1}^n s_i^T (d_i - d_C)$$
 (55)

For the first part  $\dot{V}_{l}$ , by citing the conclusion in the literature [17] there is that for any  $t \in (t_{k}, t_{k+l})$ , the following equation always holds:

$$sign(s_i(t_k)) = sign(s_i)$$
(56)

Then  $\dot{V}_i$  can continue to be reduced to:

$$\dot{V}_{I} = \sum_{i=1}^{n} \left( \eta / | s_{i} / | -k_{I} s_{i}^{T} sign(s_{i}(t_{k})) \right) = \sum_{i=1}^{n} \left( \eta / | s_{i} / | -k_{I} s_{i}^{T} sign(s_{i}) \right) 
\leq \sum_{i=1}^{n} \sum_{j=1}^{3} \left( \eta | s_{ij} | -k_{I} | s_{ij} | \right) = \sum_{i=1}^{n} \sum_{j=1}^{3} \left( \eta - k_{I} \right) | s_{ij} |$$
(57)

where j = 1, 2, 3 represents the j-th element in the vector. Combined with the range of the parameters to be designed  $0 < \eta < k_I$  it is clear that  $\dot{V}_I \le 0$ .

The second part  $\dot{V}$ , is analyzed next, substituting the robust control law (41):

$$\dot{V}_{2} = \sum_{i=1}^{n} s_{i}^{T} \left( d_{i} - d_{C} \right) = \sum_{i=1}^{n} s_{i}^{T} \left( d_{i} - \frac{d_{U} + d_{L}}{2} - \frac{d_{U} - d_{L}}{2} sign(s_{i}(t_{k})) \right) 
= \sum_{i=1}^{n} \sum_{j=1}^{3} s_{ij} \left( d_{ij} - \frac{d_{Uj} + d_{Lj}}{2} - \frac{d_{Uj} - d_{Lj}}{2} sign(s_{ij}(t_{k})) \right)$$
(58)

Discussion of (58) by case:

1) If  $s_{ij}(t_k) < 0$ ,  $sign(s_{ij}(t_k)) = -I$ , we have  $sign(s_{ij}) = -I$ ,  $s_{ij} < 0$  from (56), and combining with (40) we have:

$$\dot{V}_{2} = \sum_{i=1}^{n} \sum_{j=1}^{3} s_{ij} \left( d_{ij} - \frac{d_{Uj} + d_{Lj}}{2} + \frac{d_{Uj} - d_{Lj}}{2} \right) = \sum_{i=1}^{n} \sum_{j=1}^{3} s_{ij} \left( d_{ij} - d_{Lj} \right) < 0$$
(59)

2) If  $s_{ii}(t_k) = 0$ ,  $sign(s_{ii}(t_k)) = 0$ , while  $sign(s_{ii}) = 0$ ,  $s_{ii} = 0$ , then  $\dot{V}_2 = 0$ .

3) If  $s_{ii}(t_k) > 0$ ,  $sign(s_{ii}(t_k)) = 1$ , there is  $sign(s_{ii}) = 1$ ,  $s_{ii} > 0$ , then:

$$\dot{V}_{2} = \sum_{i=1}^{n} \sum_{j=1}^{3} s_{ij} \left( d_{ij} - \frac{d_{Uj} + d_{Lj}}{2} - \frac{d_{Uj} - d_{Lj}}{2} \right) = \sum_{i=1}^{n} \sum_{j=1}^{3} s_{ij} \left( d_{ij} - d_{Uj} \right) < 0$$
(60)

In summary,  $\dot{V}_2 \le 0$ , and the association (57) is obtained:

$$\dot{V} \le \dot{V}_1 + \dot{V}_2 \le \sum_{i=1}^n \sum_{j=1}^3 (\eta - k_1) \left| s_{ij} \right|$$
(61)

Combining the parameter range  $\eta < k_t$  yields  $\dot{V} \leq 0$ , V can converge to the sliding mode surface s. When  $\dot{V} \equiv 0$ ,  $s \equiv 0$ , the closed-loop system is asymptotically stable according to LaSalle's invariance principle, and when  $t \to \infty$ , there is  $s \to 0$ . If s = 0, the following equation holds:

$$\mathbf{s}_{i} = \mathbf{\varepsilon}_{vi} + \lambda \mathbf{\varepsilon}_{xi} = 0 \tag{62}$$

To further demonstrate that the formation cooperative position error  $\varepsilon_{xi}$  and formation velocity cooperative error  $\varepsilon_{vi}$  can also converge to 0, the Lyapunov function V' are selected as follows:

$$V' = \frac{1}{2} \boldsymbol{\varepsilon}_{xi}^T \boldsymbol{\varepsilon}_{xi} \tag{63}$$

Take the time derivate of (63)

$$\dot{V}' = \varepsilon_{xi}^T \dot{\varepsilon}_{xi} = \varepsilon_{xi}^T \varepsilon_{vi} \tag{64}$$

Combined with (62) there is:

$$\dot{V}' = \boldsymbol{\varepsilon}_{xi}^{T}(-\lambda \boldsymbol{\varepsilon}_{xi}) = -\lambda \boldsymbol{\varepsilon}_{xi}^{T} \boldsymbol{\varepsilon}_{xi} \le 0$$
(65)

Therefore, the formation cooperative position error  $\varepsilon_{xi}$  and formation velocity cooperative error  $\varepsilon_{vi}$  are asymptotically stable. When  $t \to \infty$ , there is  $s \to 0$ ,  $\varepsilon_{xi} \to 0$  and  $\varepsilon_{vi} \to 0$ . At this point, the formation will track on the desired trajectory and form the desired formation.

According to the event-triggered functions (42) and (43), the function h(t) is defined as follows:

$$h(t) = ||e_{COMM}|| = ||(\lambda - k_2)e_v - s(t_k)||$$
 (66)

By the process of proving Lyapunov stability above, it is clear that when  $t \to \infty$ ,  $e_v$  is continuous and bounded, then the following integral inequality holds:

$$||e_{COMM}|| = ||(\lambda - k_2)e_v - s(t_k)|| = ||\int_{t_k}^t \dot{e}_v(\tau)d\tau||$$

$$\leq \int_{t_k}^t ||\dot{e}_v(\tau)|| d\tau \leq k_a(t - t_k)$$
(67)

where  $k_a$  is the upper bound of  $\#\dot{e}_v \#$ .

(67) can be expressed as follows:

$$h(t) \le k_a(t - t_k) \tag{68}$$

Combined with (46) there is:

$$\lim_{t \to t_{k+l}} h(t) = \eta \le k_a (t_{k+l} - t_k)$$
 (69)

The minimum time interval  $\Delta T_{min}$  between any two trigger instants is finally obtained as:

$$\Delta T_{min} = t_{k+1} - t_k \ge \frac{\eta}{k_a} > 0 \tag{70}$$

(70) shows that the minimum time interval  $\Delta T_{min}$  is greater than 0, that is, the Zeno phenomenon will not occur.

The proof of **Theorem 1** is finished.

### 4. Numerical Simulation

In order to verify the effectiveness of the robust sliding mode formation control law based on the event-triggered strategy designed in this paper, the numerical simulation work is completed in this section, and the simulation results are analyzed. The desired tracking path of the UAV formation is an arbitrarily given spatial curve, which requires the formation to be able to form a certain formation and track on the desired path, and at the same time, the formation members communicate with each other in a discontinuous way.

The undirected graph topological communication relationship between formation members is shown in **Fig. 1**.

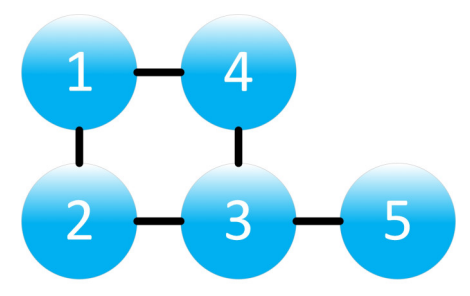


Figure 1 – UAV formation communication topology.

The formation connection matrix A is donated as

$$A = \begin{bmatrix} 0 & 1 & 1 & 0 & 0 \\ 1 & 0 & 0 & 1 & 0 \\ 1 & 0 & 0 & 1 & 1 \\ 0 & 1 & 1 & 0 & 0 \\ 0 & 0 & 1 & 0 & 0 \end{bmatrix}$$

$$(71)$$

The formation consists of five small fixed-wing UAVs, with  $m_i = 4kg$ ,  $g = 9.8 m/s^2$ . Assume that the external disturbance suffered by the *i*-th UAV is:

$$d_{iN} = 0.1[0.2\sin(0.1t), 0.2\cos(0.2t), 0.2\sin(0.2t)]^{T}$$
(72)

The initial positions, flight speeds, flight path angles and heading angles of the UAV formation members are shown in **Table 1**:

Table I illitial illiorination on OAV formation members										
UAV formation members	x -direction position (m)	y -direction position (m)	z -direction position (m)	flight speeds $V$ (m/s)	flight path angles $ heta$ (rad)	flight path angles $\psi$				
UAV1	0	0	-50	1	0.5	0.5				
UAV2	0	50	50	1	0	0				
UAV3	0	-100	0	1	0	0				
UAV4	0	100	-10	0.5	0	0				
UAV5	0	-50	-40	0.5	0	0				

Table 1 Initial information on UAV formation members

Consider the desired trajectory of the UAV formation as  $p_d = \left[40t, 10\sqrt{t}, t\right]^T$ , while five UAVs form a square formation. The formation selects UAV1 as the leader and the remaining UAVs as the

followers. The remaining parameters in the controller are selected as:  $k_1 = 1.5$ ,  $k_2 = 0.01$ ,  $\lambda = 0.8$ ,  $\eta = 0.2$ , the simulation step is 0.1s, and the simulation time is 25s. The simulation results and analyses are given below.

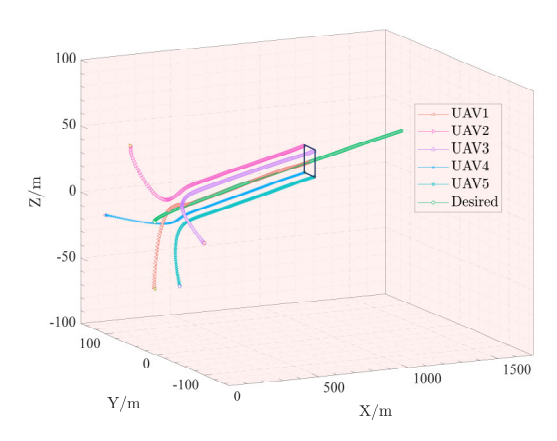


Figure 2 – UAV formation flight trajectory.

**Figure 2** shows the flight trajectory diagram of the UAV formation in three-dimensional space. As can be seen from the figure, the five UAVs start from different initial positions and then rapidly converge to the desired trajectory. After completing the formation assembly, the whole formation maintains the square formation and continues to fly along the desired trajectory.

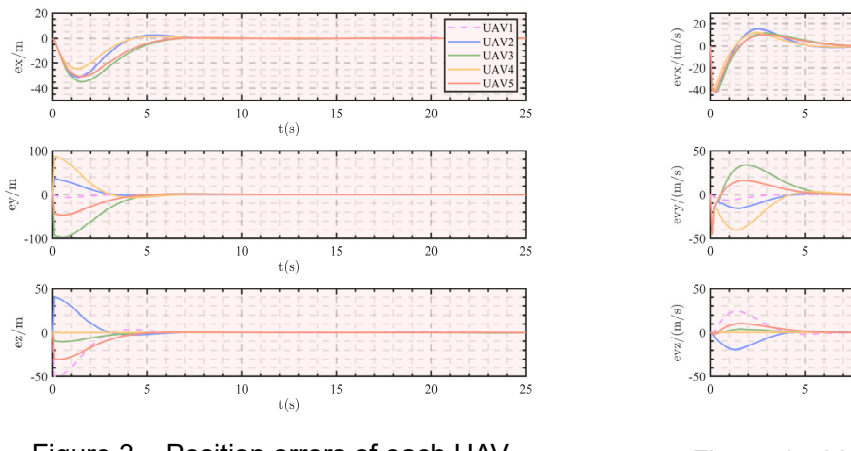


Figure 3 – Position errors of each UAV.

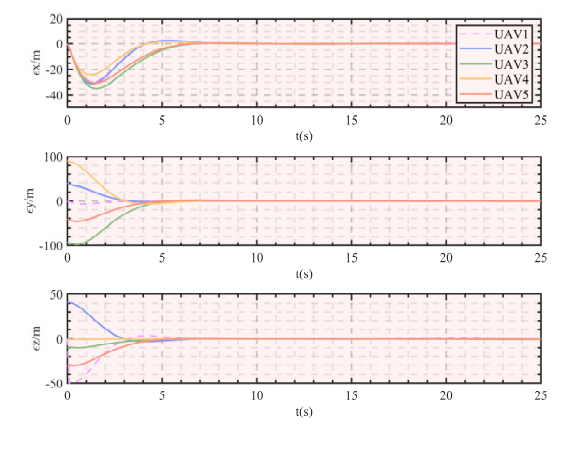


Figure 5 – Cooperative position errors.

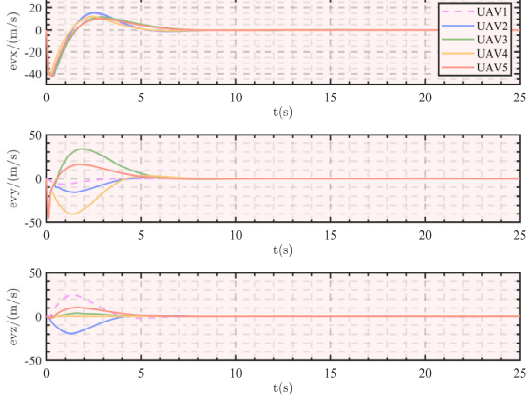


Figure 4 – Velocity errors of each UAV.

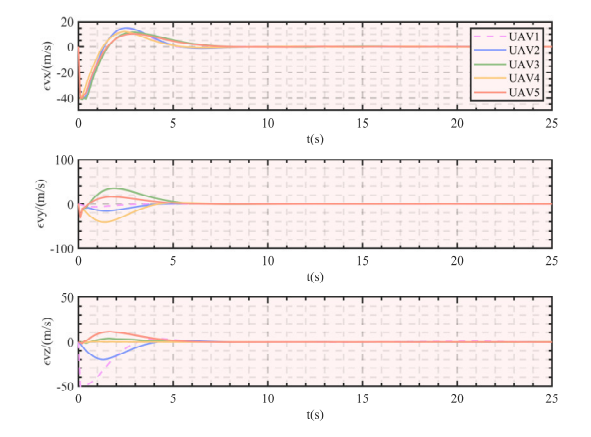
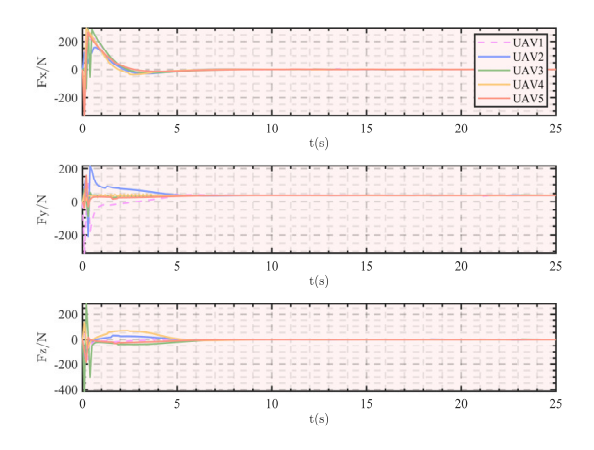


Figure 6 – Cooperative speed errors.

**Figure 3** shows the position errors, **Figure 4** shows the velocity errors, **Figure 5** shows the coordinated position errors (30), and **Figure 6** shows the coordinated velocity errors (31). From the figures, for the position and velocity errors of each member of the formation in the three directions, as well as the coordinated position error and coordinated velocity error of each UAV, all of them can be converged to the vicinity of 0 within 10s, indicating that the five UAVs, regardless of

their positions or velocities, are able to track on their respective desired trajectories, that the UAVs can complete the assemblage and form a specific formation in a relatively short period of time, and that the formation has better formation-keeping accuracy. The formation cooperative controller designed in this paper has reliable stability and good convergence speed.

Furthermore, because the formation members communicate with each other in a non-continuous manner, the event-triggered mechanism saves communication resources at the expense of system performance, which will inevitably affect the system's convergence accuracy. Based on the above error curves, it can be seen that the event-triggered formation controller designed in this paper can still guarantee the dynamic performance of the system.



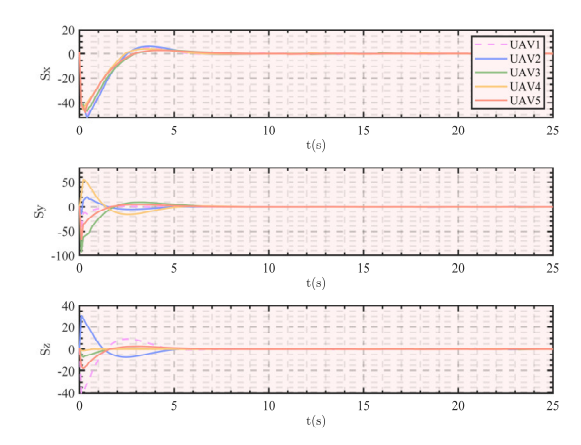
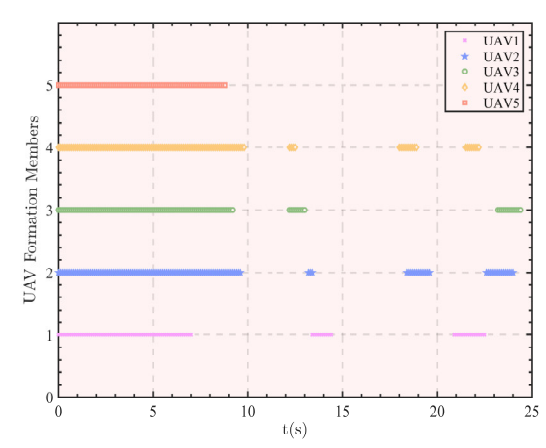


Figure 7 - Force curves of each UAV.

Figure 8 – Sliding mode surface curves.

**Figures. 7** and **8** show the control force curves and sliding mode surface curves, respectively. As can be seen from the figures, the components of the control force and sliding mode surface of each UAV in all three directions are stable within 10s. Under the update of the communication trigger moment, the sliding mode surface and control force will gradually converge to stable values.



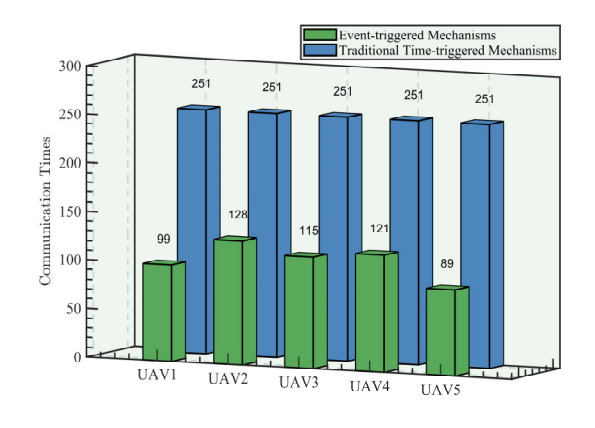


Figure 9 – Triggering instants.

Figure 10 – Communication times.

Table 2 Number of communications and percentage reduction of formation members

UAV formation members	UAV1	UAV2	UAV3	UAV4	UAV5
Number of communications	99	128	115	121	89
Percentage reduction	60.56%	49.00%	54.18%	51.79%	64.54%

**Figure 9** represents the trigger moments when the formation is in flight and the UAVs communicate with each other. Under the event-triggered communication mechanism, the formation members communicate only when the system state quantity satisfies the event-triggered condition. All five UAVs have non-contiguous communication moments.

**Figure 10** displays the communication times of each UAV in the formation and compares them to those of the time-triggered mechanism. According to the statistical graph, it can be seen that under the event-triggered mechanism, the highest number of communication times among the five UAVs is 128, and the lowest number of times is only 89. If the time-triggered mechanism is used, the

number of communication times among the UAV formation members will be as high as 251 under the same simulation time and step size.

In addition, **Table 2** gives the reduction ratio of the communication times of the event-triggered mechanism compared to the time-triggered mechanism, and the reduction ratio of the communication times of each UAV reaches up to 64.54%. If the simulation time becomes longer, the reduction ratio will increase. It can be seen that the event-triggered communication mechanism can largely reduce the number of communication times and data transmissions, reduce the communication load, and achieve the purpose of saving communication resources.

#### 5. Conclusion

For the UAV formation flight trajectory tracking problem affected by external interference and communication limitations, this paper adopts a robust controller to suppress external interference; adopts an event-triggered mechanism to achieve non-continuous communication among formation members, which greatly reduces the number of communication times and communication burdens; adopts an exponentially convergent form of sliding-mode controller to accurately control UAV formation cooperative flights, so that the UAV members can quickly form the prescribed formation; innovatively implements non-continuous communication in the case of discrete update of sliding-mode surfaces. The innovative implementation of discontinuous communication in the case of discrete update of the sliding mode surface. Through theoretical analysis, the stability proof of the closed-loop system and the exclusion of Zeno behavior are completed. The final numerical simulation results show that the proposed control scheme is effective.

# 6. Declaration of Competing Interest

The authors declare that they have no known competing financial interests or personal relationships that could have appeared to influence the work reported in this paper.

# 7. Acknowledgements

This work was supported by the China Postdoctoral Science Foundation (No. 2020 M683565), China Scholarship Council (No. 202206290159).

#### 8. Contact Author Email Address

Lihao Wang: w2019atwood@mail.nwpu.edu.cn

Aijun Li: liaijun@nwpu.edu.cn

Changqing Wang: wangcq@nwpu.edu.cn Yury Zabolotnov: yumz@yandex.ru

# 9. Copyright Statement

The authors confirm that they, and/or their company or organization, hold copyright on all of the original material included in this paper. The authors also confirm that they have obtained permission, from the copyright holder of any third-party material included in this paper, to publish it as part of their paper. The authors confirm that they give permission, or have obtained permission from the copyright holder of this paper, for the publication and distribution of this paper as part of the ICAS proceedings or as individual off-prints from the proceedings.

## References

- [1] Zhu Xiaoning. Analysis of military application of UAV swarm technology. 2020 3rd International Conference on Unmanned Systems (ICUS), Harbin, China, pp 1200-1204, 2020.
- [2] Zhang P, Huangfu H, Zhang J, Zhou J, Chen H, Tao W, Shen J, Ding Y and Su K. Formation Control of UAV Swarm Based on Virtual Potential Field and Virtual Navigator. 2021 International Conference on Big Data Analytics for Cyber-Physical System in Smart City, Shanghai, China, Vol. 1, pp 797–805, 2022.
- [3] Ouyang Q, Wu Z, Cong Y and Wang Z. Formation control of unmanned aerial vehicle swarms: A comprehensive review. Asian Journal of Control, Vol. 25, No. 1, pp 570–593, 2023.
- [4] Gu Z, Song B, Fan Y and Chen X. Design and Verification of UAV Formation Controller based on Leader-Follower Method. 2022 7th International Conference on Automation, Control and Robotics

- Engineering (CACRE), Xi'an, China, pp 38-44, 2022.
- [5] Santana L, Brandão A and Sarcinelli-Filho M. On the design of outdoor leader-follower UAV-formation controllers from a practical point of view. IEEE Access, Vol. 9, pp 107493–107501, 2021.
- [6] Liu X, Liu L, Bai X, Yang Y, Wu H, Zhang S. A Low-Cost Solution for Leader-Follower Formation Control of Multi-UAV System Based on Pixhawk. Journal of Physics: Conference Series, Vol. 1754, No. 1, pp 012081, 2021.
- [7] Yue W, Pei W, Feng L, Wei X, Run-Tang G, Fei X. Study and Practice on Control Strategy of Leader-Follower Manned-Unmanned Aerial Vehicle Formation Based on PIXHAWK Flight Control System. 2020 IEEE International Conference on Information Technology, Big Data and Artificial Intelligence (ICIBA), Chongqing, China, pp 1068-1074, 2020.
- [8] Sun Y, Shi P, Lim CC. Event-triggered sliding mode scaled consensus control for multi-agent systems. Journal of the Franklin Institute, Vol. 359, No. 2, pp 981–998, 2022.
- [9] Behera, Abhisek K and Bijnan Bandyopadhyay. Event-Triggered Sliding Mode Control for a Class of Nonlinear Systems. International Journal of Control, Vol. 89, No. 9, pp 1916–1931, 2016.
- [10]Shen S, Xu J, Chen P and Xia Q. Adaptive Neural Network Extended State Observer-Based Finite-Time Convergent Sliding Mode Control for a Quad Tiltrotor UAV. IEEE Transactions on Aerospace and Electronic Systems, Vol. 59, No. 5, pp 6360-6373, 2023.
- [11]Wang X, Yu Y, Li Z. Distributed sliding mode control for leader-follower formation flight of fixed-wing unmanned aerial vehicles subject to velocity constraints. International Journal of Robust and Nonlinear Control, Vol. 31, No. 6, pp 2110–2125, 2021.
- [12]Zhang B, Sun X, Liu S, Lv M and Deng X. Event-triggered adaptive fault-tolerant synchronization tracking control for multiple 6-DOF fixed-wing UAVs. IEEE Transactions on Vehicular Technology, Vol. 71, No. 1, pp 148-161, 2021.
- [13]Guerrero-Castellanos J, Vega-Alonzo A, Durand S, Marchand N, Gonzalez-Diaz V, Castañeda-Camacho J and Guerrero-Sánchez W. Leader-Following Consensus and Formation Control of VTOL-UAVs with Event-Triggered Communications. Sensors, Vol. 19, No. 24, pp 54-98, 2019.
- [14]Yang J, Huang X, Wu C and Mao Y. An Improved Event-Triggered Communication Mechanism with State Prediction for Multiple UAVs Formation Control. 2020 IEEE 20th International Conference on Communication Technology (ICCT), Nanning, China, pp 715-719, 2020.
- [15]Yu Z, Zhang Y, Jiang B and Yu X. Fault-Tolerant Time-Varying Elliptical Formation Control of Multiple Fixed-Wing UAVs for Cooperative Forest Fire Monitoring. Journal of Intelligent & Robotic Systems, Vol. 101, No. 48, pp 1-15, 2021.
- [16]Chen WH, Ballance DJ, Gawthrop PJ and O'Reilly J. A nonlinear disturbance observer for robotic manipulators. IEEE Transactions on Industrial Electronics, Vol. 47, No. 4, pp 932–938, 2000.
- [17]Mustafa A, Dhar NK and Verma NK. Event-triggered sliding mode control for trajectory tracking of nonlinear systems. IEEE/CAA Journal of Automatica Sinica, Vol. 7, No. 1, pp 307–314, 2020.